IMPACT OF THE PRE-CHAMBER NOZZLE ORIFICE CONFIGURATIONS ON COMBUSTION AND PERFORMANCE OF A NATURAL GAS ENGINE

by

Xianyin LENG[a], Mei WANG[b], Zhixia HE[a*], Qian WANG[b], Shengli WEI[c], Wuqiang LONG[d], and Chuangen ZHU[e]

[a]Institute for Energy Research, Jiangsu University, Zhenjiang, Jiangsu, China
[b]School of Energy and Power Engineering, Jiangsu University, Zhenjiang, Jiangsu, China
[c]School of Automotive and Traffic Engineering, Jiangsu University, Zhenjiang, Jiangsu, China
[d]Institute of Internal Combustion Engine, Dalian University of Technology, Dalian, China
[e]Shengli Oil Field, Shengli Power Machinery Group Company LTD, Dongying, Shandong, China

Original scientific paper
https://doi.org/10.2298/TSCI170912008L

In this study, a pre-chamber was designed to form near stoichiometric mixture and provide multiple turbulent flame jets to ignite the lean mixture and accelerate the combustion in the main combustion chamber for a natural gas engine. A CFD simulation was employed to investigate the impact of the pre-chamber nozzle configurations on flow and combustion processes inside the engine, as well as on the performance of the engine. Various configurations were investigated, including orifice number of 4 to 8 and orifice diameter ranging from 1.6 m to 2.9 mm. A non-dimensional parameter, β, was used to characterize the relative flow area of these configurations. The numerical results indicate that, for a given nozzle flow area, among the design of different orifice numbers, the 6-orifice design can obtain the optimal combustion and engine performance. Otherwise, a design of more orifices leads to slower flame penetrating speed in the main-chamber, and the design of less orifices leads to slower circumferential flames propagations in the main-chamber. Moreover, for a 6-orifice pre-chamber, the optimal orifice diameter was found to be 2.0 mm, corresponding to a β value of 0.3. A design of larger diameters leads to slower penetrating for the flame jets and insufficient radial flame propagations in the main-chamber, while a design of relatively smaller orifice diameters leads to insufficient circumferential flames propagations in the main-chamber. Additionally, for the engine performance, all the pre-chamber designs improve the indicated efficiency and reduce the NO_x emission. Especially, the design of 6-orifice with diameter of 2.0 mm achieves a 35.0% increase of indicated thermal efficiency and a 78.0% reduction of NO_x emission compared to the prototype engine.

Key words: *orifice geometry, pre-chamber, flame jets, spark plug, β value, natural gas engine*

Introduction

Due to the rising cost of crude oil and stringent emission regulations, natural gas has become a promising alternative clean fuel for internal combustion engines due to its advantages in fuel costs, fuel economy and pollutant emissions [1-3]. At present, most gas engines

* Corresponding author, e-mail: zxhe@ujs.edu.cn

operate at stoichiometric combustion mode, using homogeneous mixture with the equivalence ratio of around 1.0. This combustion mode leads to low thermal efficiency and high pollutant emissions, as well as high knocking tendency [4]. Combustion of a lean air-fuel mixture in a spark ignition (SI) engine is one method to reduce the NO_x emissions and it increase engine efficiency by decreasing a peak combustion temperature. On the other hand, increasing the excess air leads to the increase in emissions of HC, but especially causes a large reduction in engine performance expressed by a decrease in the maximum indicated mean effective pressure and maximum torque. A SI pre-chamber stratified combustion system has the potential to improve or overcome these problems. On one hand, stoichiometric mixture can be formed in the pre-chamber by an independent fueling system, resulting in a reliable ignition and stable combustion inside the pre-chamber. On the other hand, when the pre-chamber flame propagates into the main-chamber through orifices, the turbulent flame jets become high energy igniters for the lean mixture in the main-chamber. These flame jets energy are greatly higher than that from a spark igniter, thus they can ignite very lean mixture. Moreover, the intensive turbulences induced by the flame jets will accelerate the combustion in the main-chamber and improve the combustion stability. Therefore, pre-chamber stratified combustion system is one of the most effective ways in expanding lean-burn ability and improving gas engine performance [5]. Almost all of the major global automotive companies conducted, or maintained, the work on a two-stage combustion process stratified mixtures in engine with pre-chamber (Honda, Porsche). Currently, most automotive SI engines with stratification fuel mixture by altering the design of the combustion chamber does not allow the reduction of toxic emissions to the level imposed by the European and American standards. The preparation and combustion of stratified mixtures in engines equipped with pre-chamber was abandoned and the fuel direct injection to the single combustion gasoline direct injection (GDI) chamber was introduced. Currently, lean combustion by a pre-chamber charge stratification is applied mostly in stationary supercharged gaseous engines of medium and high power operating at constant rotational speed which are focused mainly on the use of stationary electricity production and gas compression [5].

One of the first attempts to research of effectiveness of lean mixtures ignition and combustion in the engine with the pre-chamber was the system called the pilot flame torch ignition system. This system patented in 1963 by Gussak *et al*. (see in [1]). The lean mixture combustion system with a small chamber for ignition was also subject of studies conducted by Oppenheim's group since 1978 in Berkeley, University of California. Then, a number of researches have been conducted to understand such combustion behaviors. The G46 type engine of MAN B&W [6] and the 46 DF type engine of Wartsila [7] both adopted the pre-chamber combustion system, which both obtained a thermal efficiency of higher than 46%. The J920 type natural gas generator set of JE Jenbacher Company obtained a thermal efficiency of 50% and very NO_x emissions [8]. For these pre-chamber engines, the geometrical structure of the pre-chamber and the orifices between the pre- and main-chamber plays a significant role on gas-flow and flame propagation behaviors. In some cases, even a subtle change in the orifice geometry may lead to a notable change in combustion characteristics and engine performances [4]. Therefore, a thorough investigation on the structure of pre-chamber and orifices is necessary for optimizing engine performances.

The aim of this paper is to find the optimal number and diameter of the orifices between the pre- and main-chamber of a Shengdong T190 type natural gas engine which is used for stationary electricity production. The investigation was performed by CFD simulation using CONVERGE package. Several designs of the orifice geometries were numerically accessed and an optimal design was acquired.

Description of the CFD approach

Numerical models

The flow and combustion processes of the natural gas fueled engine were calculated using the CFD package Converge v2.1. The turbulent behaviors of the flow field were calculated using a RNG k-ε model [9]. This two equation RANS model is derived based on a mathematical technique called *renormalization group* method. Since this model considers the streamline bending, swirl, rotation and fast changing tension effects, it is especially suitable for the complex flow field, such as the gas-flow in an internal combustion engine. The SAGE detailed chemistry solver was employed for using detailed chemical kinetics in combustion simulations with a set of CHEMKIN-formatted input files which can define chemical mechanism. The GRI mechanism for methane combustion, which consists of 52 species and 261 reactions [10], was adopted in the calculation. Moreover, the SI processes were described with the AKTIM model. While the NO_x formation was predicted using the Zeldovich model in [11]. To accelerate the solution of detailed chemical kinetics, the multi-zone model was employed with a 2-D zoning strategy.

Geometrical models and meshing strategies

Specifications of the Shengdong T190 natural gas engine are listed in tab. 1. This prototype T190 engine works at stoichiometric combustion mode with a spark plug. In this study, pre-chamber and orifices were designed to implement stratified lean combustion mode, while the geometries of the main-chamber, intake and exhaust ports remained unchanged. A non-dimensional parameter, β, [12] was employed to characterize the pre-chamber orifices. This parameter represents for the relative flow area of orifices and penetration of flame jet. It is defined as:

$$\beta = \frac{BAt}{Vpcc} \tag{1}$$

where B is the bore of the engine cylinder, At – the orifice flow area, and $Vpcc$ – the pre-chamber volume. In this study, the pre-chamber volume was designed to be 3% of the compression volume.

A schematic view of the pre- and main-chamber geometries system is presented in fig. 1. The geometrical model includes the intake and exhaust ports, pre-chamber, orifices, spark plug, and the main-chamber. The spark plug was set in the top center of the pre-chamber. Various orifice structures for the pre-chamber were designed, providing different numbers and

Table 1. The specifications of Shengdong T190 engine

Items	Parameters
Stroke	210 mm
Bore	190 mm
Cylinder number	12
Connecting rod	410 mm
Compression ratio	11:1
Number of valves	4
Power	700 kW
Speed	1000 rpm
Displacement volume	71.45 L
Ignition advance angle	20 °CA

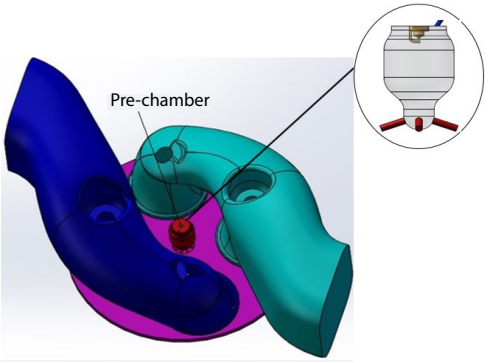

Figure 1. The geometrical model of the gas engine

diameters (β values) of the orifices, as listed in tab. 2. These cylindrical orifices uniformly distributed around the pre-chamber, which was located at the axis of the cylinder. The including angle among these orifices was kept at 140°. As presented in tab. 2, totally 25 cases were performed to investigate the effects of orifice number and orifice on the combustion characteristics. In this paper, only two parts of the results were selected to be reported. After obtaining the results of all cases, the optimal orifice number and β value were determined. Then, the results corresponding to different orifice number under the optimal β value and different orifice diameters under the optimal orifice number were discussed.

Table 2. The list of various orifice structures

	$\beta = 0.2$	$\beta = 0.3$	$\beta = 0.4$	$\beta = 0.5$	$\beta = 0.6$
4-orifices	2 mm	2.5 mm	2.9 mm	3.2 mm	3.6 mm
5-orifices	1.8 mm	2.2 mm	2.6 mm	2.9 mm	3.2 mm
6-orifices	1.6 mm	2 mm	2.4 mm	2.7 mm	2.9 mm
7-orifices	1.5 mm	1.9 mm	2.2 mm	2.4 mm	2.68 mm
8-orifices	1.4 mm	1.76 mm	2.04 mm	2.3 mm	2.5 mm

An adaptive mesh refinement (AMR) technique was employed for the meshing of the calculating domain. After a mesh independent study, the following mesh strategies were determined. Firstly, a relatively coarse meshing with grid size of $4 \times 4 \times 4$ mm was defined as the base grid. Then, the spatial resolutions of regions having high temperature or velocity gradients will be automatically increased, with a refinement level of up to 3, *i. e.*, minimum mesh size of 0.5 mm. In addition, fixed embedding method should be applied to refine the critical regions. In this study, a fixed embedding region with refinement level of 5 was set for a sphere region round the spark plug gap, providing grid resolution of 0.125 mm, as shown in fig. 2. Moreover, the refinement level of 2 and 3 were set on the whole pre-chamber region and pre-chamber orifices region, respectively. Figure 3 shows the computed grid for the engine combustion chambers. Under theses meshing strategies, the cell number during the calculation was found to be ranging from 0.3 to 1.2 million. The temporal resolutions were determined by the maximum allowed Courant Friedrichs-Lewy numbers, providing variable time stepping. The maximum convective and diffusive CFL number was set as 1.0 and 0.5, respectively.

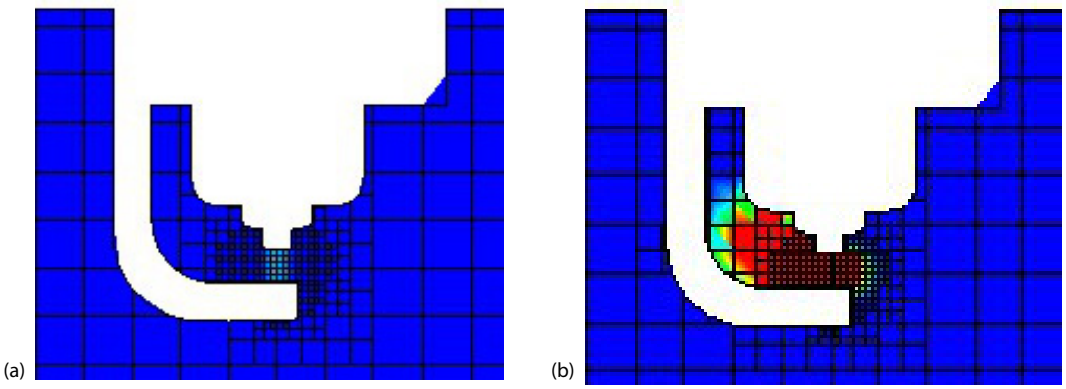

Figure 2. The meshes around the spark plug electrode; (a) the meshes around the spark plug electrode at ignition timing (b) the meshes around the spark plug electrode 2° crank angle degree after the ignition timing

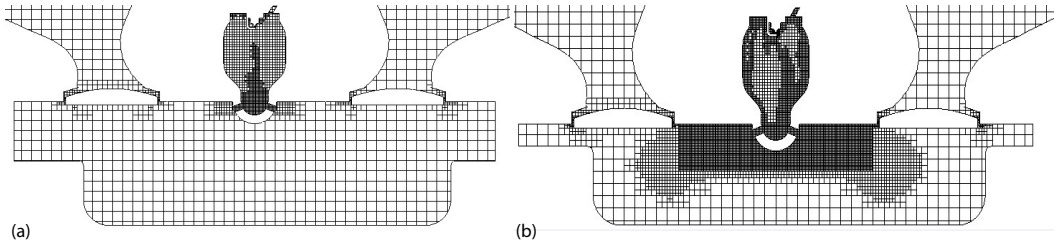

Figure 3. The computed grid for the engine combustion chambers; (a) the grid before ignition timing (b) the 12° crank angle degree after the ignition timing

Initial and boundary conditions

The simulation began at the intake valve open timing (330 °CA) and ended at the exhaust valve open timing (840 °CA). As previously described, the model included four regions including the intake ports, the exhaust ports, the main-chamber and a pre-chamber. Different initial and boundary conditions established by GT-Power were set for these regions. The boundary conditions were listed in tab. 3. The initial temperature and pressure in the cylinder, pre-chamber and the exhaust port were set at 850 K and 0.25 MPa, respectively. While that of the intake port were set at 318 K and 0.2 MPa. Furthermore, a homogeneous lean mixture with equivalence ratio of 0.5 was initially set inside the intake port, as well as at the inlet boundary, to provide lean mixture in the main-chamber. During the gas exchange stage, a near stoichiometric mixture will be formed in the pre-chamber with appropriate fuel enrichment injection strategies.

Table 3. The boundary conditions

Boundary	Temperature [K] Pressure [MPa]
Piston, liner, cylinder head	450 K
Pre-chamber	450 K
In (pre-chamber)	350 K
Spark plug	550 K
Spark plug electrode	950 K
Exhaust port	830 K
Outflow	800 K, 0.25 MPa
Exhaust valve	930 K
Intake port	330 K
Inflow	330 K, 0.25 MPa
Intake valve	480K

The CFD simulation for the in-cylinder combustion process of the prototype T190 engine at 100% load was conducted. The comparison between computational and experimental in-cylinder pressure and heat release rate (HRR) profiles are shown in fig. 4. It can be seen that the predicted and experimental pressure and the HRR profiles are in good agreement throughout the compression and combustion stages. With an error of about 0.1 MPa, the peak in-cylinder pressure and its phase have been predicted acceptably. Moreover, the discrepancies between the predicted and measured HRR are within an allowable range. In addition, the predicted indicated specific NO_x emission is 7.06 g/kWh, which is a little lower than the measured value (7.72 g/kWh). It may be due to the fact that as a result of numerical modelling, NO emission

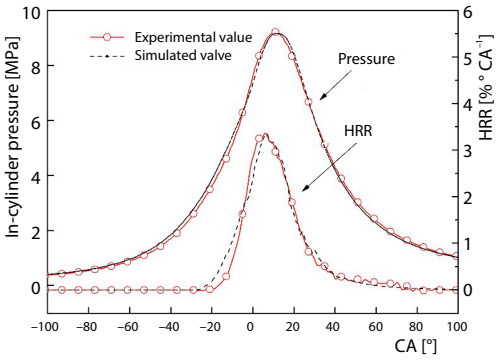

Figure 4. The comparison of in-cylinder pressure and normalized HRR

is obtained, while NO_x emissions are measured during experimental research. NO_x mainly consists of NO and NO_2. The NO_2 is formed outside the cylinder by oxidation of NO in atmospheric air. Overall, it could be concluded that a moderately good agreement has been achieved, and the adopted mechanism and models are capable to represent the combustion process of natural gas engines.

Results and discussion

The effects of the orifice number on the combustion characteristics

Figure 5 shows the temporal variations of the flame temperature distribution for the five designs with different orifice number at constant β value of 0.3. For each group of contours, the upper one presents the results at the vertical section, while the lower one presents the results at the horizontal section at 2 mm under the cylinder head. During the compression stroke, parts of the lean mixtures in the main-chamber flow into the pre-chamber through the orifices, forming different turbulent structures in the pre-chamber that further influences the combustion and the turbulent flame jets. As seen from the temperature contours in the figure, at 6 °bTDC, the high-speed flame jets have been propagated from the pre-chamber to the main-chamber. The penetration of the flame jets for the various orifice number cases differs due to the different

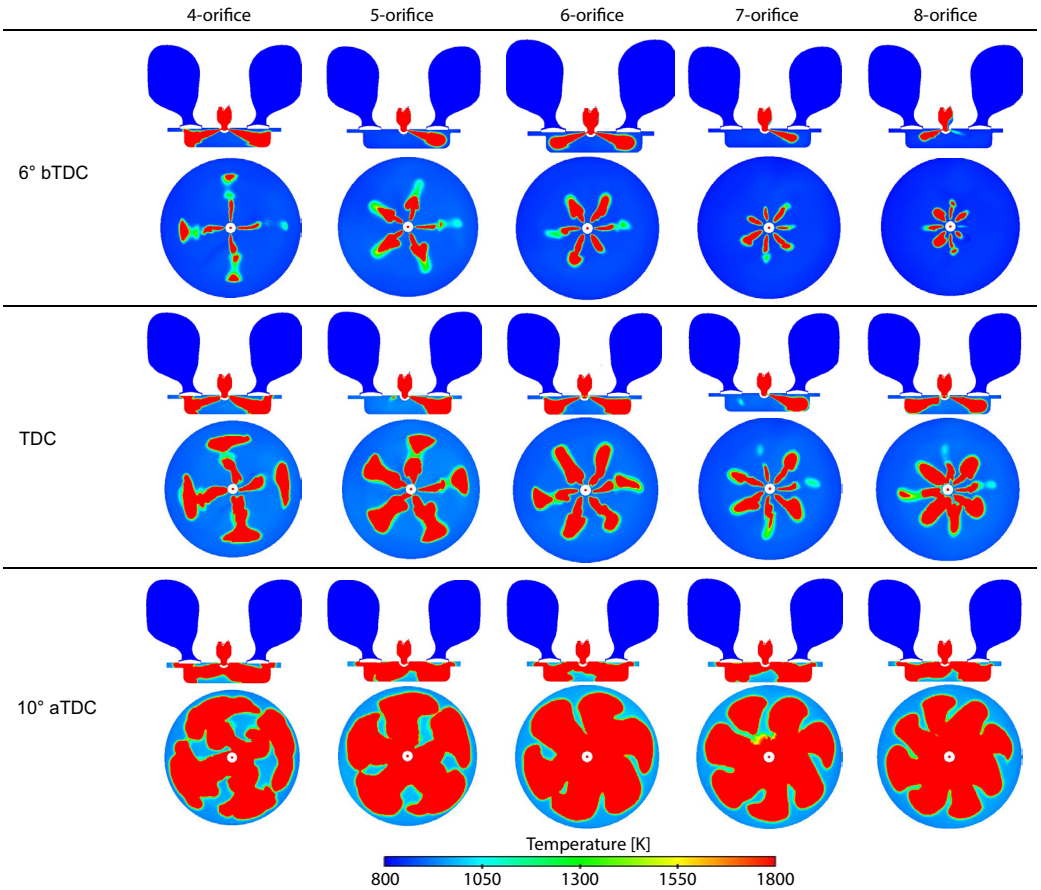

Figure 5. Temperature contours in the main-chamber with the design of various orifice numbers (*for color image see journal web site*)

jet velocities and pressure. For the case of similar number of orifices, the different flame jet distances observed were as a result of the turbulence in main-chamber. From the lateral cross--sectional view, it is clearly seen that, the flame jets from the 4-orifice case have the longest penetration, followed by 5-orifice and 6-orifice cases. The flames of the 4-orifice design reach the edge of the piston bowl, and start to develop to the top of the piston. While the flame jets from the 8-orifice design are still at the upper center region of the chamber bowl. At TDC, there was a significant increase in the flames at the cross-sectional area. The 4-orifice design, obtained the longest radial flame jets. However, there is large area of non-combustion zones due to the less number of orifice.

The 8-orifice case had the shortest radial flame jets lower flame velocity and pressure, leading also to a large non-combustion circumferential zone in the main-chamber. The 5-orifice case and 6-orifice designs obtained the minimum non-combustion zones. At 10 °aTDC, the flame profiles from each orifice were almost uniform when the influences of turbulence in the main-chamber were not so obvious. The non-combustion zones of the 4-orifice case and the 5-orifice case were still very large due to the less number of orifice. While the 7- and 8-orifice cases result in insufficient radial flame jet penetrations. Thus, it is clear that the 6-orifice design achieved the minimum non-combustion zone. However, the design of excessive orifices leads to insufficient radial propagation of flames in the main-chamber, and the design of less orifices leads to insufficient circumferential flames propagations in the main-chamber.

Figure 6 shows the numerical results of averaged jet velocities at the exits of these pre-chamber orifices. Here, positive value means from the pre- to main-chamber. It can be seen that the 4- and 8-orifice case has the highest and lowest jet velocity, respectively. With the increasing of the orifice number, the velocity of the flame jets tends to reduce. This trend is in agreement with the different flame jet penetrating velocity for different orifice number designs shown in fig. 5.

To have a better understanding of the combustion characteristics, the pressure and HRR *vs*. CA for the design with different orifice numbers were compared as shown in fig. 7. From the pressure curve, it is clear that the pre-chamber pressure curve for all cases have double peaks: the first peak correspond to the rapid combustion of the near stoichiometric mixture inside the pre-chamber, while the second peak is a result of pressure rising in the main- -chamber, which also propagated to the pre-chamber. The start of combustion (SOC) phasing in the

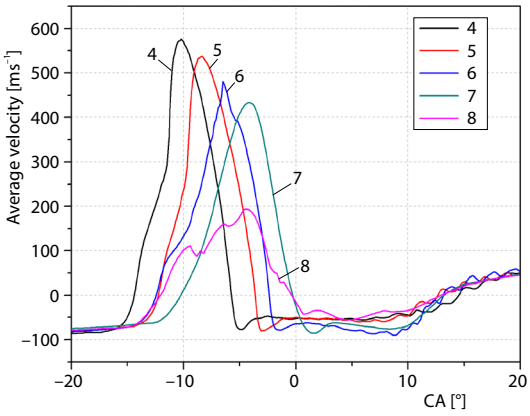

Figure 6. The average velocity of jets from pre-chamber orifices to cylinder

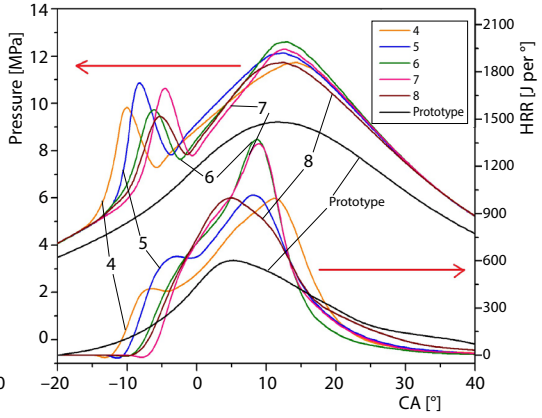

Figure 7. The pressure in pre-chamber and HRR in the main-chamber for various orifice numbers

pre-chamber for each cases were different, due to the different turbulent structures and mixture distributions determined by the orifice geometries. These differences can further affect the lean burn in the main-chamber. The 4-orifice case obtained the most advanced SOC in the pre-chamber but shows a relatively lower in-cylinder pressure and HRR, which is mainly due to the lower number of orifice leading to insufficient circumferential flame propagation. The 8-orifice case also exhibits quite low in-cylinder pressure and HRR, which can be attributed to the insufficient radial flame penetrating rater due to the lower jet velocity. As it can be seen, the 6-orifice case acquires the highest in-cylinder pressure (12.8 MPa) and HRR (1485 J/°CA) at around 10 °aTDC, followed by the 7-orifice case. Moreover, the HRR curve of the 6-orifice case is narrower than the ones obtained for the other cases. That is, it has the highest gradient in the ascending and descending phases of HRR. Therefore, it can be concluded that, with the 6-orifice number case, the relatively higher combustion rate resulted in shorter combustion duration.

As known, thermal NO_x is the dominant mechanism for the NO_x formation in an internal combustion engine, which is highly dependent on combustion temperature, oxygen concentration and retention time. Therefore, thermal NO_x was adopted to calculate the NO_x formation in this study. Figure 8 presents the predicted NO_x emission for designs of various orifice numbers. It is noted that for all cases, the indicated specific NO_x emission are at around 1.2 g/kWh, which are extremely lower than that of the prototype engine (7.06 g/kWh). It could be attributed to the much lower flame temperature of the lean burn mode, as shown in fig. 5, the maximum combustion temperature in the main-chamber is around 1800 K. Moreover, the orifice number also affects the NO_x emission. The 6-orifice number design results in the highest NO_x emission. This is most probably related to its very high combustion rate. Consequently, other designs which yield lower combustion rate obtain slightly lower NO_x emission.

The variation of unburned hydrocarbons (UHC) emissions in the exhaust gases depends on the quality of combustion process in cylinder. There are several reasons for UHC emissions in this study. On one hand, the premixed mixture in the main-chamber is very lean, which leads to insufficient oxidation or even extinction in the cylinder. On the other hand, a lean mixture flame weakens and extinguishes when it propagates to the locations near the cylinder wall and piston crevices. Figure 8 presents the effect of orifice number on UHC emissions. It can be seen that the UHC emissions are slightly lower for the 6-orifice design than those of the other designs. This is mainly due to the fastest flame propagation and optimal combustion process in cylinder for the design of this orifice number. Higher or less number of orifice restrains the flame propagation, resulting in slightly higher UHC emissions.

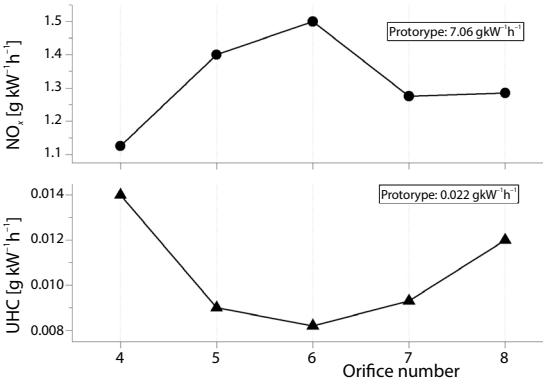

Figure 8. The NO_x emission and the mass of UHC under various orifice number

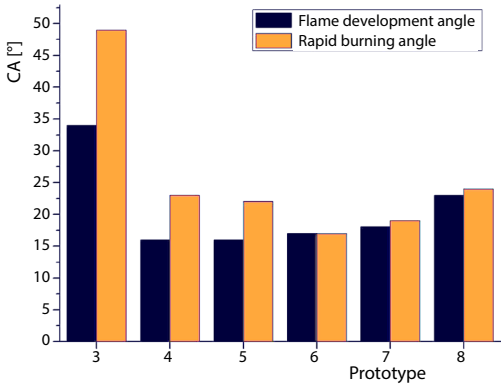

Figure 9. Combustion duration of various orifice number

Figure 9 shows the comparison of combustion duration for the design of various orifice numbers. It should be noted that flame development duration refers to the time from spark timing to 10% of the fuel been burned (CA10) in the main-chamber, while rapid combustion duration is from CA10 to CA90 in the main-chamber [13]. It is obviously from the figure that, the flame development duration is approximately 16 °CA for all the cases except for the 8-orifice case. The 6-orifice case has the shortest rapid burning duration of about 17 °CA and the overall combustion duration, while the 8-orifice case has the longest combustion duration.

Based on the previous discussion, it can be concluded that the orifice number of the pre-chamber has significant effects on the gas-flow and combustion process in the pre- and main-chamber. Under the constant β value, excessive orifices will lead to insufficient radial flame propagations in the main-chamber due to inadequate jet velocity and pressure, which will further prolong the combustion duration. On the other hand, lesser number of orifice will lead to insufficient circumferential flame propagation in the main-chamber. Although the flame jet penetration are sufficient, circumferential propagations of the flames require a longer time, thereby prolonging the combustion duration. The 6-orifice case obtained the highest rate of flame propagation and NO_x emissions. Since the highest NO_x emission is still much lower than that from the prototype engine, moreover, the differences of NO_x emission among these cases are not quite large, the optimal orifice number in this study is considered to be 6.

The effects of the orifice diameter on the combustion characteristics

To obtain the optimal orifice diameter under the 6-orifice design, the effects of orifice diameter on combustion characteristics is presented in this section. Table 4 shows the various diameters with the β value ranging from 0.2-0.6.

Table 4. Various diameters under 6-orifice design

β	0.2	0.3	0.4	0.5	0.6
Diameter [mm]	1.6	2	2.4	2.7	2.9

Figure 10 shows the lateral and axial cross sectional views of the temperature distribution in cylinder (for example, at 6 °bTDC, the upper picture is a lateral cross-sectional view and the lower one is an axial cross-sectional view) of the main-chamber at various orifice diameters (1.6-2.9 mm) under the constant orifice number. Larger or smaller orifice diameters were found to be not good for flame propagation. At 6 °bTDC, there are no significant differences among the flame profiles from the lateral sectional views. The 6 flames appeared in main-chamber as seen from the axial cross-sectional views. The flame penetrations are longer for β value of 0.3 and 0.4. Also the shortest flame penetration is obtained when the β value is 0.6. At the TDC, there are significant increases in the circumferential flame area as seen from the figure, especially at β values of 0.5 and 0.6 due to the larger orifice diameter. Although, the non-combustion zones are still very big due to low jet velocities and short radial flame jet distances, the relatively smaller orifice diameter cases obtained the minimum circumferential flame areas. At β value of 0.4, the flames attained the minimum non-combustion zones due to the relatively larger circumferential areas and longer radial flame jet distances. At 10 °aTDC, the minimum non-combustion zone is attained when β value is 0.4, followed by the case of β value is 0.3, while the maximum non-combustion zone is attained by the largest orifice diameter case ($\beta = 0.6$) as a result of shorter flame jet distances. Therefore, relatively larger or smaller orifice diameters would hinder combustion and prolong the combustion duration. Figure 11 shows the temporal evolution of the pre-chamber pressure and HRR in the main-chamber for all the orifice diameter cases. From the pressure curve, it can be seen that the SOC positions are different. When β value are 0.2, 0.5, and 0.6, relatively more advanced SOC in the pre-chamber are

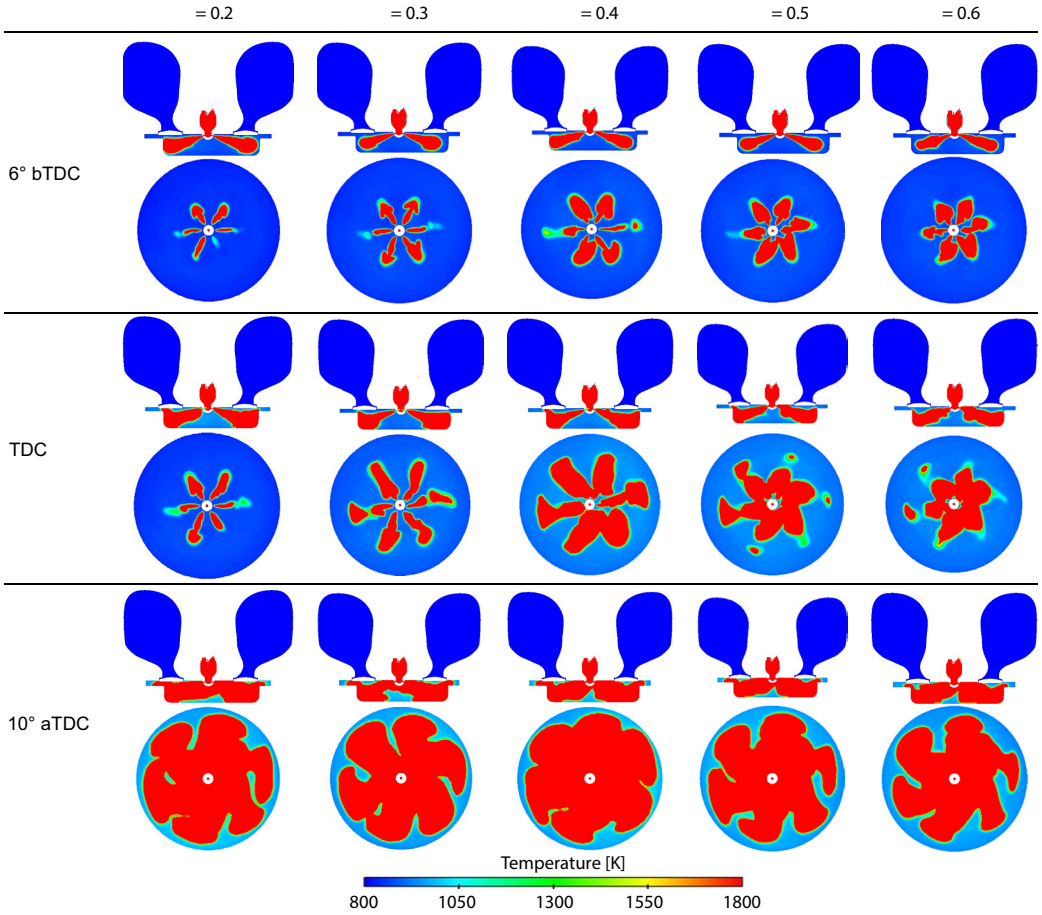

Figure 10. Temperature contours in chamber under various β value
(*for color image journal see web site*)

obtained, together with relatively lower in-cylinder pressure and HRR. This is mainly caused by the insufficient circumferential or radial flame propagation due to the size of the orifice diameters (either relatively smaller or bigger). As can be seen, when the β value is 0.4, the highest in-cylinder pressure (13 MPa) and HRR (1385 J/°CA) at around 8 °aTDC after top dead center, are attained. Moreover, the HRR curve of this design is narrower than the ones obtained for the other cases, which implies a much higher combustion rate. However, the extremely high HRR usually associated with knocking. Therefore, the design with β value of 0.3 is selected as the optimal case, which provides almost the same level of thermal efficiency (almost identical main-chamber pressure curve), while the HRR is considerably lower than the design with β value of 0.4.

Figure 12 shows the NO_x emissions for the design of different orifice diameters. When β value is 0.4, the lowest gross indicated specific NO_x emission (1.8 g/kWh) is attained due to high temperature. However, 76% reduction of NO_x emission is achieved when compared to the prototype engine. The lowest emissions (1.43 g/kWh) are achieved at the β value of 0.3. Figure 12 also shows the mass of UHC under various β value. It can be seen that the UHC emissions is much lower when the β value is 0.4 compared to that of other β values. Figure 13 shows com-

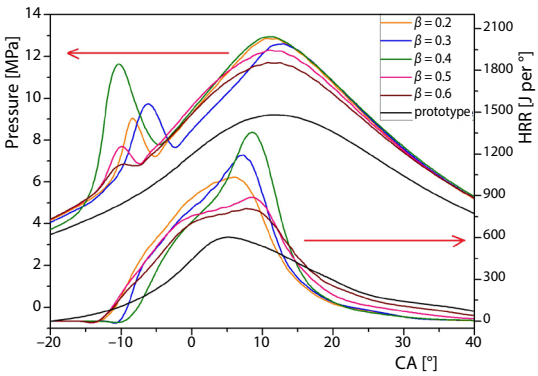

Figure 11. The pressure in pre-chamber and HRR in the main-chamber under various β value (*for color image see journal web site*)

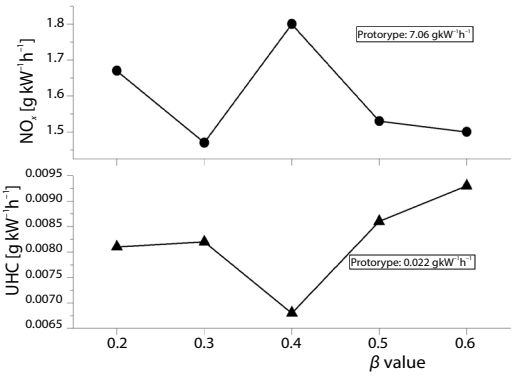

Figure 12. The NO_x emission and the mass of UHC under various β value

bustion duration comparison under all the orifice diameters. It can be seen all orifice diameter cases have shorter combustion duration than the prototype engine. At β value of 0.4, the shortest flame development and rapid burning durations of 14 °CA is obtained. The smallest orifice diameter case has the longest flame development duration of about 18 °CA, while the largest orifice diameter case has the longest rapid burning duration of about 28 °CA. Eventually, the highest combustion rate is obtained with the medium orifice diameter when β is 0.4, followed by the design with a β of 0.3, which results in a reasonable rapid combustion rate. While the lowest combustion rate is obtained by the largest diameter case.

Figure 14 shows the comparison of gross indicated power and the gross indicated thermal efficiency of the designs with various orifice diameters. It is clear that the engine performances attained from all the pre-chamber cases are much better than the ones from the prototype engine. At β value of 0.3, the indicated power and indicated thermal efficiency of about 95 kW and 57% were obtained, respectively. Resulting in a 35.0% higher indicated thermal efficiency than that of the prototype engine.

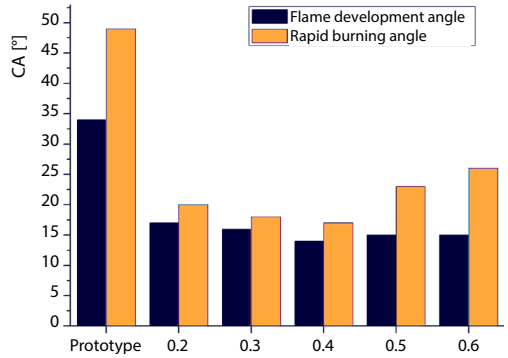

Figure 13. Combustion duration under various β value

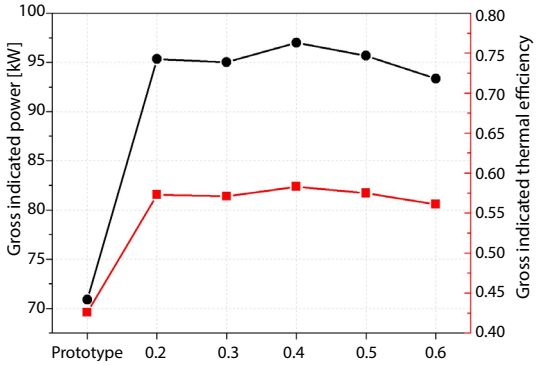

Figure 14. Comparison of gross indicated parameters for various β value

From the previous discussions, it can be concluded that optimal value is required for the pre-chamber orifices diameter. Immoderately large or small orifice diameters have negative effects on combustion characteristics in the cylinder. Under constant orifice number, larger diameters lead to short flame jet distances and insufficient radial propagations of the flames in the

main-chamber due to insufficient jet pressure. This further prolongs the combustion duration. Furthermore, smaller orifices diameters lead to insufficient circumferential propagation of the flames in the main-chamber. This also requires more time, hence prolonging the combustion duration. In this paper, the optimal orifice diameter determined is 2 mm at the β value of 0.3. Very high flame propagation rate and short combustion duration was obtained under this set of parameters. The result corresponds to the ones obtained in research studies of Watson [14].

Conclusions

Based on the numerical investigations conducted, the following conclusions, relating to the effects of orifice geometry between pre- and main-chamber of a natural gas engine, were observed as follows.

- The pre-chamber number of orifices have significant effects on gas-flow and combustion in pre- and main-chambers. Under a constant β value, higher number of orifices leads to insufficient radial propagation of flames in the main-chamber, hence prolonging combustion duration further. Also insufficient number of orifices leads to insufficient circumferential flames propagations in the main-chamber, which also prolongs the combustion duration. The optimal orifice number attained is 6.
- The pre-chamber orifice had an optimal diameter with regards to the number of orifices attained. Relatively larger or smaller diameter have negative effects on combustion processes. Larger diameters leads to short penetration for the flame jets and insufficient radial flames propagations in the main-chamber due to insufficient jet pressure. This prolongs the combustion duration. Relatively smaller orifice diameters leads to insufficient circumferential flames propagations in the main-chamber, also prolonging the combustion duration. The optimal orifice diameter is 2 mm at β value of 0.3. With this parameters, the higher rate of flame propagation and the shorter combustion duration was obtained.
- Finally, the optimized geometrical structure of the orifices was found to be a combination of 6-orifices with 2 mm diameter. With this, a 35.0% increase of indicated thermal efficiency and a 78.0% reduction of NO_x emission was achieved as compared to the prototype engine.

Acknowledgment

This research was supported by the Natural Science Foundation of Jiangsu Province (Grant No. BK20130514, BK20161349); National Natural Science Foundation of China (Grant No. 51776088); a Project Funded by the Priority Academic Program Development of Jiangsu High Education Institutions; Senior Professionals Scientific Research Foundation of Jiangsu University (Grant No. 12JDG080); Top six talents in Jiangsu Province (Grant No. JXQC-010).

References

[1] Jamrozik, A., *et al*., Numerical Simulation of Two-Stage Combustion in SI Engine with Prechamber, *Applied Mathematical Modelling*, *37* (2013), 5, pp. 2961-2982
[2] Shah, A., *et al*., Effect of Relative Mixture Strength on Performance of Divided Chamber Avalanche Activated Combustion Ignition Technique in a Heavy Duty Natural Gas Engine, SAE technical paper, 2014-01-1327, 2014
[3] Douailler, B., *et al*., Direct Injection of CNG on High Compression Ratio Spark Ignition Engine: Numerical and Experimental Investigation, SAE technical paper, 2011-01-0923, 2011
[4] Shah, A., *et al*., CFD Simulations of Pre-Chamber Jets' Mixing Characteristics in a Heavy Duty Natural Gas Engine, SAE technical paper, 2015-01-1890, 2015
[5] Toulson, E., *et al*., A Review of Pre-Chamber Initiated Jet Ignition Combustion Systems, SAE technical paper, 2010-01-2263, 2010

[6] Boeckhoff, N., Mogele, H., Improvement & New Applications of the MAN 51/60 Gas Engine for Marine & Power plant, *Proceedings*, 27th World Congress, Shanghai, China, 2013, CIMAC paper, p. 294
[7] Watanabe, K., *et al*., Update on Wartsila 4-Stroke Gas Product Development, *Proceedings*, 27th World Congress, Shanghai, China, 2013, CIMAC paper, p. 406
[8] Christian, T., *et al*., GE's All New J920 Gas Engine a Smart Accretion of Two-Stage Turbocharging, Ultra Lean Combustion Concept and Intelligent Controls, *Proceedings*, 27th World Congress, Shanghai, China, 2013, CIMAC paper, p. 289
[9] Gao, J., *et al*., Numerical Study on Spray and Mixture Stratified Combustion in a Direct Injection Gasoline Engine, *Transactions of CSICE*, *4* (2005), 23, pp. 296-306
[10] Zesty, E., *et al*., Reduction of a Detailed Kinetic Model for the Ignition of Methane/Propane Mixtures at Gas Turbine Conditions Using Simulation Error Minimization Methods, *Combustion and Flame*, *158* (2011), 8, pp.1469-1476
[11] Li, S. S., *et al*., Influence of Pre-Chamber Parameters on Combustion Process in Large Natural Gas Engine, *Chinese Internal Combustion Engine Engineering, 6* (2012), 33, pp.72-76
[12] Kirkpatrick, A., *et al*., CFD Modeling of the Performance of a Pre-Chamber for Use in a Large Bore Natural Gas Engine, *Proceedings*, ASME ICES Conference, Chicago, Ill., USA, 2005, ICES2005-1049
[13] Heywood, J. B., *Internal Combustion Engine Fundamentals*, International edition, McGraw-Hill, New York, USA, 1988
[14] Watson, H., *et al*., Optimizing the Spark Ignition Pre-Chamber Geometry Including Spark Plug Configuration for Minimum NO_x Emissions and Maximum Efficiency, *Proceedings*, 19th International Fisita Congress, Melbourne, Australia, 1982, p. 131

Paper submitted: September 12, 2017
Paper revised: December 29, 2017
Paper accepted: January 6, 2018